

Aeroacoustic resonance in a rectangular cavity: Part 2 Effect of yaw and of leading and trailing edge angles

S. M. Henbest¹, M. B. Jones¹, A. Blandford¹ and J.H. Watmuff²

¹DSTO, 506 Lorimer Street, Fishermans Bend, 3207, Melbourne, Australia

²School of Mechanical and Manufacturing Engineering, RMIT, Bundoora, 3083 Australia

Abstract

Experimental results of flow over a generic “open” rectangular cavity having lengths of 200 and 250 mm and a depth and width of 50mm at Mach numbers ranging between 0.3 to 1.3 was reported in Part 1 [1]. In this paper, Part 2, the effect of yawing these rectangular cavities is investigated, as well as how the yawing resonant behaviour changes when the shorter cavity is transformed to a range of parallelograms by changing the leading and trailing edge angles while keeping the length to depth and width ratios fixed. The results show that small leading and trailing edge angles changes of up to 15° have a small influence on resonance behaviour and for the two largest angles, 30° and 45°, the magnitude of resonances are suppressed at a zero yaw.

Introduction

The effect of yaw upon the behaviour of resonant tones has had significantly less interest than work looking at passive and active techniques for suppressing high intensity acoustic modes that can occur in rectangular cavities. In the early 1990s, initial work Tracy *et al.* [2] and Plentovich *et al.* [4] investigated the effect of yaw angle, $\beta = 0^\circ$ and 15° , upon the static pressure distribution in “open” rectangular cavities with length to depth (L/D) ratios of 4.4 & 6.7, and in “closed” cavities with L/D ratios of 12.67 & 20.0, over a range of subsonic and transonic Mach numbers. For definitions of open and closed cavity flows see [4]. They varied the cavity depth to achieve their specified L/D values. Their reported upstream boundary layer thickness was approximately 12.7mm. This work was extended in [3] to include spectral information on the observed resonance modes and they compared these to the predicted values derived from a modified form [6] of Rossiter’s equation [5]. They noted that for their $L/D = 4.4$ cavity, the “open” cavity behaviour at $\beta = 0^\circ$ changed to “open/transitional” behaviour at $\beta = 15^\circ$. They reported that similar resonances were observed at both angles indicating the aero-acoustic feedback mechanism was not significantly changed. Coincidentally, their cavity - 285.75 mm long, 63.5 mm wide - was of a similar scale to the cavities tested here.

Experimental method

The experimental arrangement described in Part 1 [1] had the $L/D = 5$ cavity mounted in a turntable which allowed the flow yaw angle, β , to be varied through $\beta = \pm 90^\circ$. Hence the opportunity existed to repeat the measurements of [3] and hopefully provide further quantification of the effects of yaw upon both the frequency and magnitudes on the observed resonance modes. As will be shown, the results from the yawed $L/D = 5$ cavity highlighted particular changes in the resonance behaviour near and above a yaw angle of $\beta = 15^\circ$. At $\beta = 15^\circ$ the leading and trailing edges are inclined 15° to the normal to the flow and the axis of the cavity is inclined 15° to the flow. The authors were interested in the resonance behaviour of this $\beta = 15^\circ$ case and decided that leading and trailing edge inserts inclined at -15° would return the front and rear cavity walls to be aligned normal to the flow with

the axis and side walls of the cavity remaining at the angle $\beta = 15^\circ$ as shown in figure 1. The cavity in Part 1 [1] was modified to accept leading and trailing edge inserts with a mean axial length of 25 mm each and this reduced the effective cavity length to 200 mm giving an $L/D = 4$. Five leading and five trailing edge inserts were manufactured with the following angles 0, 5, 15, 30, and 45 degrees. For the tests reported here, by using leading and trailing edge inserts with similar angles, the cavity geometry was modified to be rectangular or a parallelogram with angles of 5, 15, 30 and 45 degrees. The experimental measurement method and analysis techniques used are the same as described in Part 1 [1], namely Kulite pressure transducers are flush mounted on the bottom face, port and starboard walls of the cavity. Three basic sets of results are presented here for Mach numbers of 0.5, 0.7, 0.9, 1.1 and 1.3 at a tunnel pressure of 120 kPa as follows:

1. $L/D = 5$ rectangular cavity for yaw angles $\beta = 0^\circ, 5^\circ, 10^\circ, 15^\circ, 20^\circ, 25^\circ, 30^\circ$.
2. $L/D = 4$ rectangular cavity for yaw angles $\beta = 0^\circ, 5^\circ, 10^\circ, 15^\circ, 20^\circ, 25^\circ, 30^\circ$.
3. $L/D = 4$ parallelogram cavities (5, 15, 30 and 45 degrees) for varying yaw angles from $\beta = -30^\circ$ through to $+30^\circ$ in 5° intervals.

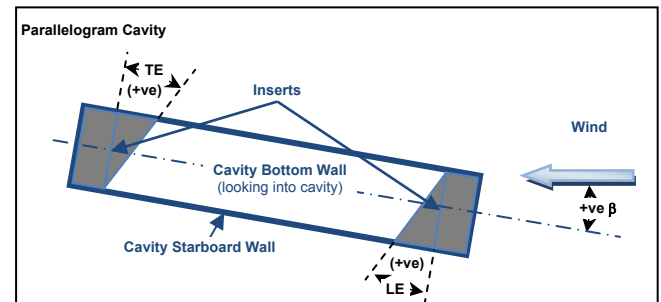


Figure 1. Schematic of $L/D = 4$ yawed parallelogram cavity defining leading and trailing edge orientation.

Experimental Results - Rectangular Cavity $L/D = 4$ & 5

Non-dimensional power spectral density of pressure fluctuations

Figure 2 show the normalised fluctuating pressure power spectral density versus the normalised frequency, Strouhal number, for discrete values of $\beta = 0^\circ, 5^\circ, 10^\circ, 15^\circ, 20^\circ, 25^\circ, 30^\circ$ plotted as a contour plots, one for each Mach number 0.5, 0.7, 0.9 and 1.1. The Kulite pressure sensor was located at $x/L = 0.9$ on the centreline of the floor in the $L/D = 5$ rectangular cavity.

In these plots the calculated Rossiter modes [5] are shown as dashed vertical lines. Examination of the data shows the dominant mode is the second; the next most dominant is the first and only at higher Mach numbers is the third mode evident. The behaviour of the modes with yaw angle is interesting. Considering the $M = 0.5$ case first, as the yaw angle increases to

10°, the frequency of the second mode decreases slightly and its magnitude increases and at $\beta = 10^\circ$ the first mode becomes stronger. At $\beta = 15^\circ$ the first mode diminishes considerably and the second mode frequency jumps up and the third mode now becomes dominant. At $\beta = 10$ and 15° , the low frequency components also evident and are not associated with any Rossiter mode. At yaw angles $\beta = 20^\circ$ and above, all resonances are suppressed. For $M = 0.7$ these trends are not so evident. However, at the two highest Mach numbers, $M = 0.9$ and 1.1 , similar behaviour to the $M = 0.5$ case is observed; additionally, the third mode is seen at $\beta = 0^\circ$, disappears at 10° and reappears at $\beta = 15, 20$ and 25° but with a lower frequency.

Figure 3 shows similar contour plots for the rectangular $L/D = 4$ cavity and in this case the Kulite transducer was located at $x/L = 0.875$. There are several differences between the $L/D = 4$ and $L/D = 5$ data. Firstly, the magnitude of the non-dimensional

PSD is significantly less for the $L/D = 4$ cavity compared to the $L/D = 5$ cavity. Secondly, the decrease of the second mode frequency with increasing yaw angle is exacerbated in the $L/D = 4$. Thirdly, the peak in the second mode PSD extends to a higher value of $\beta = 15^\circ$ and the jump in frequency occurs at $\beta = 20^\circ$. The differences in the features that are observed between the $L/D = 4$ data compared to the $L/D = 5$ data at similar yaw angles are likely due to the small geometric difference, one being that the diagonal angle of the cavity is 14.0 and 11.3 degrees, respectively. In other words, not unexpectedly, when the yaw angle exceeds the diagonal angle of a cavity the resonance spectral behaviour also changes.

Figure 4 shows the pressure coefficient, C_p , data of Plentovich *et al* [3] in an $L/D = 4.4$ rectangular cavity at $M = 0.9$ for $\beta = 0$ and 15 degrees. Their $L/D = 4.4$ cavity had a length of 11.25 inches and a width of 2.50 inches and this corresponded to a diagonal angle of 12.52 degrees. Their C_p distribution at $\beta = 0^\circ$ was typical of an “open” cavity while at $\beta = 15^\circ$ (an angle greater than the diagonal value) the C_p distribution was no longer typical of an “open” cavity and was shown to be more characteristic of a “transitional/open” type of cavity flow. The current $L/D = 4$ cavity C_p distributions for $M = 0.9$ are also shown in the figure. In our case, the cavity length was 200 mm and the width 50 mm and this corresponded to a diagonal angle of 14.03 degrees. The current $L/D = 4$ results show that the C_p distributions appear to be more typical of an “open” cavity, however; as β increases the distribution does change towards that characteristic of a “transitional/ open” cavity, indicating a weak change in flow structure may have occurred; though the magnitude of the change is less than observed in the $L/D = 4.4$ cavity data of [3]. At $\beta = 20^\circ$ (an angle greater than the $L/D = 4$ diagonal angle) the change in the C_p distribution is the greatest. At the other Mach numbers, the C_p behaviour is similar to that in figure 4 with the differences being slightly greater at lower Mach numbers. The C_p observations are consistent with the changes in spectral behaviour shown in figures 2 and 3 at $\beta = 15$ and 20° and may be hypothesised to be associated with flow structure changes for yaw angles β near or greater than the diagonal angle of the cavity.

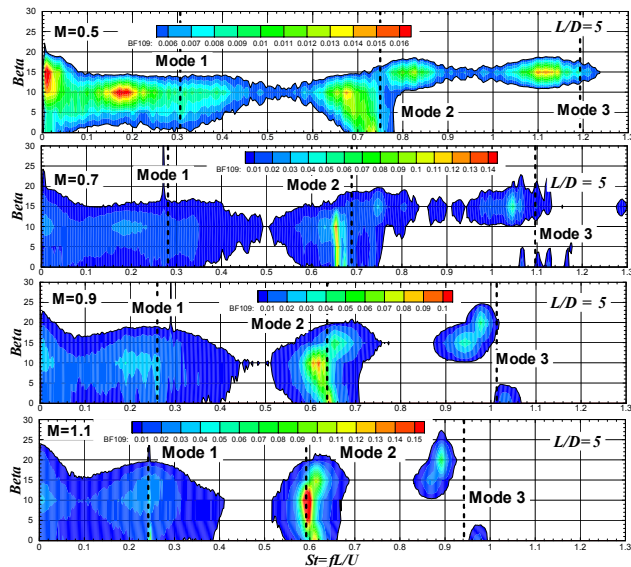


Figure 2. Contour plots of the non-dimensional fluctuating pressure power spectral density versus Strouhal number, St , and the angle of yaw β . The Kulite measurement transducer was located at station on the floor centreline at $x/L = 0.9$ of $L/D = 5$ cavity. Contour plots are shown for four Mach numbers, $0.5, 0.7, 0.9$ and 1.1 .

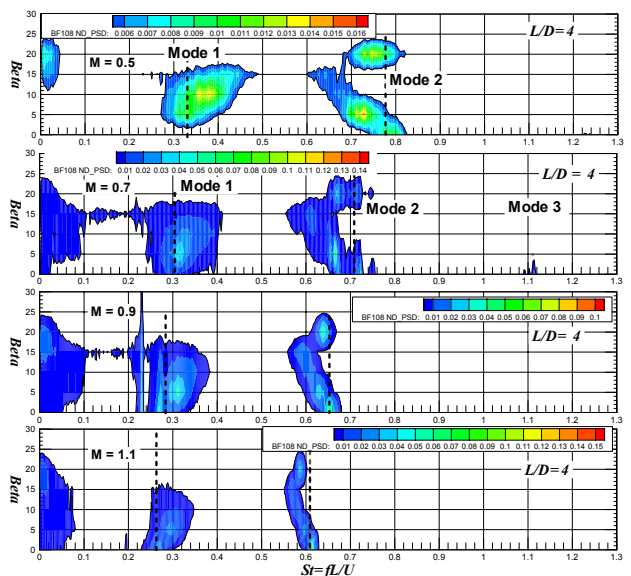


Figure 3. Contour plots of the non-dimensional power spectral density versus Strouhal number (St) and angle of yaw (β) for $M = 0.5, 0.7, 0.9$ and 1.1 . The Kulite measurement transducer was located at on the centreline of the floor of $L/D = 4$ cavity at $x/L = 0.875$.

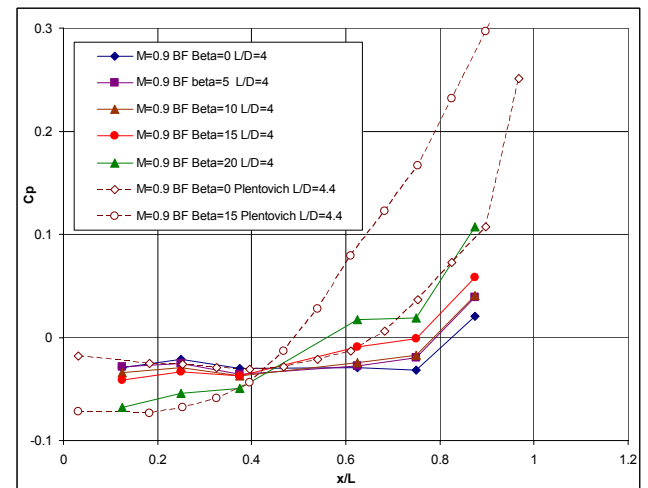


Figure 4. Variation in C_p distributions along the floor centreline of rectangular cavities for varying yaw angle β at $M = 0.9$. Current data for $L/D = 4$ shown together with data of Plentovich [3] for $L/D = 4.4$.

Effect of yaw upon dominant resonant mode magnitudes and frequencies

As noted previously, mode 2 was primarily the dominant mode for both $L/D = 4$ and 5 cavities. Figure 5 shows the $L/D = 4$ variations in the non-dimensional PSD over limited discrete Mach number values for different yaw angles. For the baseline

case of $\beta = 0^\circ$, the second mode non-dimensional PSD peak value increased monotonically with M ; at $\beta = 5^\circ$ the magnitude at $M = 0.7$ exceeds the baseline value and then diminishes at higher Mach number, at 10° the magnitudes are suppressed the most, increase at 15° and at 20° return to magnitudes close to baseline values.

Effect of yaw upon resonant mode frequencies

Figure 6 shows plots of the ratio of frequency at a given yaw angle normalised by the baseline frequency at a yaw angle of $\beta = 0^\circ$ for a given Mach number. Mode 2 frequency behaviour is shown in figure 6(b). At $M = 0.5$ this frequency ratio decreases monotonically with increasing yaw angle and at 15° the frequency has reduced to 80% of the baseline value, further increases in yaw angle 20 and 25° see the ratio return closer to the baseline frequency. This trend of decreasing frequency with increasing yaw angle up to 15° persists for the higher Mach numbers, however; the relative change in frequency decreases as the Mach number increases and appears to asymptote to single distribution for the highest three Mach numbers (0.9, 1.1 and 1.3). This behaviour is different to that observed by [2] and [3], also shown in figure 6(b), which showed a small or no change in the frequency ratio.

For mode 1 shown in figure 6(a), the frequency behaviour is the opposite, that is at $M = 0.5$ the frequency ratio increases with increasing yaw angle and reaches a value of 145% at 15° . Once again the effect diminishes with increasing Mach number and there is no systematic trend. Frequency ratio data for mode 3 is shown in figure 6(c) for consistency, the authors point out that there is neither sufficient data nor are the magnitudes large enough to draw any firm conclusions.

The authors at this stage do not have any physical explanation as to why the frequency of mode 2 decreases and of mode 1 increases as yaw angle increases up to the diagonal angle of the cavity. Flow visualisation studies may assist in the interpretation. Applying a narrow band filter centred about each mode frequency to the pressure signals and further signal processing could provide an indication as to whether mode 1 or mode 2 behaviour is dominant to assist interpretation of the images.

Experimental Results – Parallelogram Cavities $L/D = 4$

Effect of leading and trailing edge angles.

Figure 7 show the normalised fluctuating pressure power spectral density versus the normalised frequency (St) and yaw angle (β from -25° to $+30^\circ$) as contour plots. The Kulite pressure sensor was located at $x/L = 0.875$ on the centreline of the floor in the $L/D = 4$ cavity.

Figure 7(a) shows the contours at $M = 0.7$ for the rectangular cavity and the four leading/trailing edge angle combinations. Compared to the rectangular cavity, the 5 degree inserts make little difference to the contour plots and a small degree of asymmetry is introduced. For the 15 degree inserts, the energy in mode 1 extends to slightly higher positive values of yaw and for mode 2, the peak PSD value occurs at $\beta = 5^\circ$ with the resonance also extending to slightly higher yaw values. Similar frequency behaviour as noted in figure 6 occurs, that is mode 1 frequency increases and mode 2 decreases with yaw angle. Only with the 30 and 45 degree inserts are there significant changes to the resonance behaviour of the cavity. For the 30 degree inserts, at $\beta = 0^\circ$ mode 1 and mode 2 are both slightly suppressed, the peak value for mode 2 now occurs around $\beta = 15^\circ$. The distribution is asymmetric and for negative yaw angles the resonance is no longer clearly apparent. For the 45 degree inserts

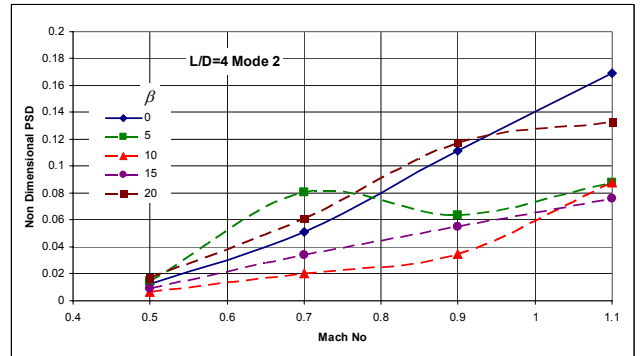


Figure 5. Mode 2 peak non-dimensional PSD magnitude versus Mach number for varying angles of yaw β measured at $x/L = 0.875$ in the $L/D = 4$ rectangular cavity.

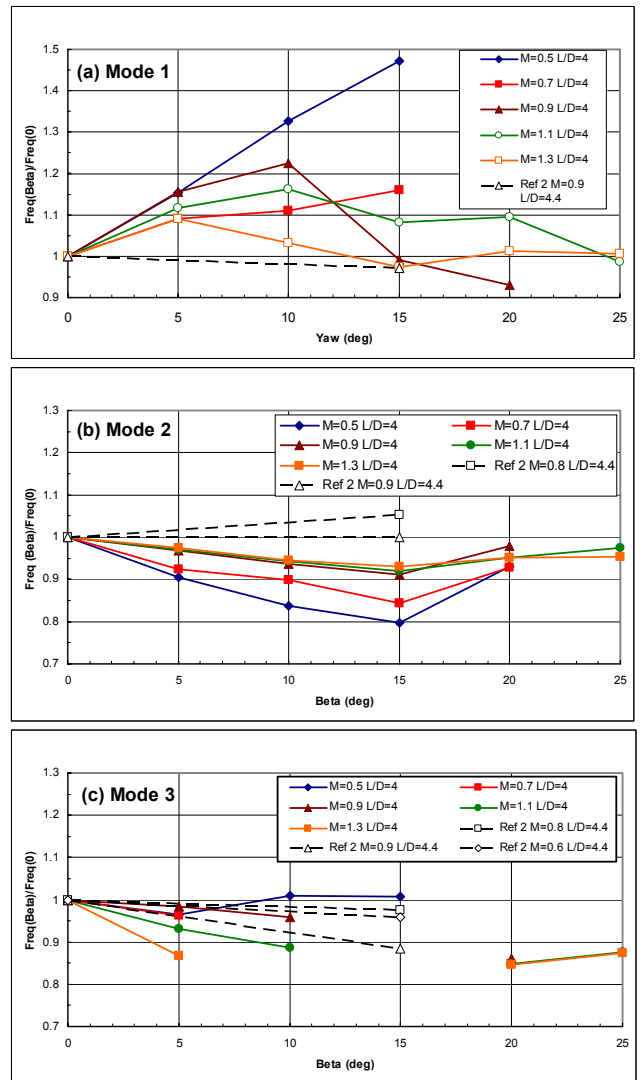


Figure 6. Frequency normalised by frequency at $\beta = 0$ versus yaw angle β for $L/D = 4$ rectangular cavity over a range of Mach Numbers (a) Mode 1, (b) Mode 2, (c) Mode 3. Also shown is the data of [2] for $L/D = 4.4$.

the resonance behaviour has moved to be centred about a yaw angle of range $+10^\circ$ to $+15^\circ$ with no resonance apparent at values of $\beta \leq 0^\circ$. The data for $M = 1.1$ is shown in figure 7(b) and here the resonance behaviour is similar to the $M = 0.7$ cases. At higher Mach numbers the bandwidth of the second mode is narrower and more clearly defined. The broad conclusion is that 5 and 15

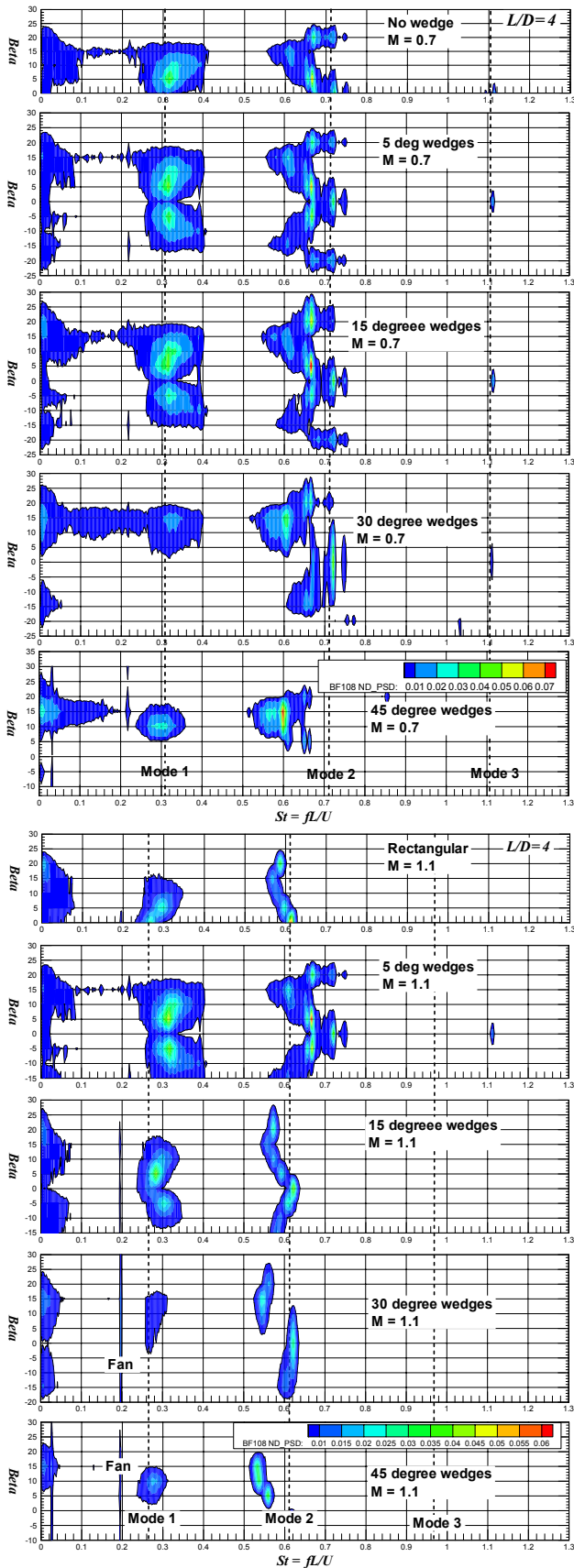


Figure 7. Contour plots of the non-dimensional pressure PSD versus Strouhal number (St) and the angle of yaw (β) for $L/D = 4$ parallelogram cavities with varying leading and trailing edge angles of 0, 5, 15, 30 and 45 degrees. (a) $M = 0.7$ and (b) $M = 1.1$.

degree inserts have limited influence on the resonance. The observed changes in resonance with yaw may be associated with

cross flow relative to the side walls as well as relative to the diagonal of the cavity.

Conclusions

Experiments to measure the fluctuating pressure spectrum in rectangular cavities of length to depth ratios of 4 and 5 have been conducted for varying discrete angles of yaw and over a Mach number range of 0.5 to 1.3. The second mode is observed to be the most dominant; as the yaw angle increases the second mode frequency decreases; at yaw angles slightly above the diagonal angle of each cavity, the second mode frequency returns to a value slightly less than the zero yaw angle condition and with further increase in yaw all resonance modes disappear. In contrast, the frequency behaviour of the first mode increases with increasing yaw angle. Measured static pressure distributions show that for yaw angles less than the diagonal angle of the cavity the pressure distribution is characteristic of an “open” cavity flow, however; for yaw angles near or greater than the diagonal angle the pressure distribution is more characteristic of an “transitional/open” cavity flow.

Leading and trailing edges inserts of 0, 5, 15, 30 or 45 degree were used to form five parallelogram cavities where the front, back and side walls all remained normal to the top and bottom of the cavity. Only with the 30 and 45 degree inserts were there significant changes to the spectral resonance behaviour.

The authors do not have a physical explanation as to why the frequency of the second mode decreases and of the first mode increases as yaw angle increases up to the diagonal angle of the cavity. At yaw angles less than the diagonal angle of the cavity the cavity flow remains “open” and for yaw angles greater than the diagonal angle in the cavity flow becomes more “transitional/open” than “open”. The authors recommend that the rectangular cavity measurements be repeated with greater resolution in yaw angle to investigate more carefully the change in cavity flow behaviour at the yaw angles close to the diagonal angle of the cavity.

Acknowledgments

The authors wish to acknowledge QinetiQ for modifications to experimental rig and the support of DSTO technical and professional staff in the running of experiments.

References

- [1] Henbest, S. M., Jones, M. B., Watmuff, J. and Blandford, A., Aeroacoustic resonance in a rectangular cavity: Part 1 Effect of Mach and Reynolds number, in *18th Australasian Fluid Mechanics Conference, 2012*.
- [2] Tracy, M. B., Plentovich, E. B. and Chu, J., Measurements of fluctuating pressure in a rectangular cavity in transonic flow at high Reynolds numbers, Tech. Rep. *NASA-TM-4363, NASA, 1993*.
- [3] Plentovich, E. B., Chu, J. and Tracy, M. B., Effects of yaw angle and Reynolds number on rectangular box cavities at subsonic and transonic speeds, *Tech. Rep. NASA TP-3309, NASA, 1991*.
- [4] Plentovich, E.B., Stallings, R.L. and Tracy, M.B. Experimental cavity pressure measurements at subsonic and transonic speeds, *NASA Tech Paper 3358, 1993*.
- [5] Rossiter, J. E., Wind-tunnel experiments on the flow over rectangular cavities at subsonic and transonic speeds., *ARC Reports and Memoranda 3438, Aeronautical Research Council, 1964*.
- [6] Heller, H. H., Holmes, D. G. and Covert, E. E., Flow induced pressure oscillations in shallow cavities, *Journal of Sound and Vibration, 18, 1971, 545–546*.